

Inclusive Pion Double Charge Exchange in ${}^4\text{He}$

E. R. Kinney and J. L. Matthews

Massachusetts Institute of Technology, Cambridge, Massachusetts 02139

P. A. M. Gram, D. W. MacArthur, and E. Piasetzky^(a)

Los Alamos National Laboratory, Los Alamos, New Mexico 87545

and

G. A. Rebka, Jr., and D. A. Roberts

University of Wyoming, Laramie, Wyoming 82071

(Received 4 August 1986)

The pion spectra observed in the inclusive double-charge-exchange reactions ${}^4\text{He}(\pi^+, \pi^-)4p$ and ${}^4\text{He}(\pi^-, \pi^+)4n$ are strikingly different from those in heavier nuclei, exhibiting a prominent peak at high outgoing pion energies. The shapes of these spectra, while qualitatively consistent with two sequential single-charge-exchange processes, are not yet quantitatively understood.

PACS numbers: 25.80.Fm, 25.10.+s, 27.10.+h

Inclusive pion double charge exchange (DCX) is a direct probe of multistep pion-nucleus processes, as conservation of charge requires that DCX involve at least two nucleons. The simplest mechanism by which this reaction can proceed consists of two sequential single charge exchanges [e.g., $n(\pi^+, \pi^0)p$ followed by $n(\pi^0, \pi^-)p$]. Several calculations¹⁻³ of DCX cross sections based on this mechanism have been performed for ${}^3\text{He}$ and ${}^4\text{He}$. More exotic mechanisms, such as double-charge-exchange scattering of the incident pion by the pion cloud surrounding the nucleons,^{3,4} or virtual pion production and reabsorption,⁵ have also been considered. However, previous experimental investigations of DCX in ${}^4\text{He}$ have been limited to searches for a tetraneutron bound state,⁶ and a few other measurements at isolated energies and angles.⁷⁻⁹ The paucity of systematic data has hampered comparison of theory with experiment and prevented a decisive choice among these models.

A systematic experimental study of inclusive DCX in ${}^4\text{He}$, the lightest nucleus which can support both (π^+, π^-) and (π^-, π^+) reactions, has been undertaken over a broad range of incident energies encompassing the $\Delta(1232)$ resonance. The reaction ${}^4\text{He}(\pi^+, \pi^-)4p$ was observed at incident energies 120, 150, 180, 240, and 270 MeV. At each incident energy, the doubly differential cross section was measured at three to five angles between 25° and 130° over the entire range of outgoing pion energies from 10 MeV up to the kinematic limit for the reaction in which the final state consists of the oppositely charged pion plus four free nucleons.

The experimental procedure was essentially identical to that followed in our previous measurements of DCX in ${}^{16}\text{O}$ and ${}^{40}\text{Ca}$.^{10,11} Pion fluxes of up to 10^9 s^{-1} from the high-energy pion channel at the Clinton P. Anderson Meson Physics Facility (LAMPF) impinged on 326 mg cm^{-2} of liquid helium contained in a thin-walled (50-

μm Mylar) vertical target cylinder (2.5 cm in diameter \times 8 cm high) at atmospheric pressure. Background from the target walls was generally less than 5% except at the lowest incident pion energy, where a background of up to 30% was measured. Pions were detected by a 180° , 60-cm-radius, double-focusing spectrometer instrumented with a wire chamber between its two 90° dipoles and a focal-plane array consisting of a pair of wire chambers, a plastic scintillation counter, and two threshold Čerenkov detectors, one with a fluorocarbon (FC-88) radiator, the other with an Aerogel ($n = 1.055$) radiator. In the absence of pion-induced pion production, detection of a pion with charge opposite to that of the incident pions is a unique signature of DCX.

To obtain absolute cross sections, the beam-flux monitors were calibrated for each incident beam energy and charge by our observing pion-proton elastic scattering from a Styrofoam (CH) target of the same configuration as the liquid-He target and comparing the measurement with the prediction of an accepted phase-shift representation of the $\pi^\pm p$ cross section.¹²

As a sample of the ${}^4\text{He}(\pi^+, \pi^-)4p$ measurements, the doubly differential cross section for $T_{\pi^+} = 240$ MeV and $\theta_{\pi^-} = 25^\circ$ is shown in Fig. 1(a). The errors indicated here, and in all subsequent figures, represent the statistical uncertainty in each observation plus the energy-dependent systematic uncertainties (symbols without bars are larger than the uncertainties); overall systematic errors in the absolute values of the cross sections are approximately 10%. A possible "background" contribution from pion-induced pion production has not been subtracted, and for 240 MeV can contribute to the yield of outgoing pions with energies below 75 MeV. This background is estimated to be less than 12% of the total cross section at this incident energy and much smaller at lower energies.

For comparison, the spectrum observed in the reaction

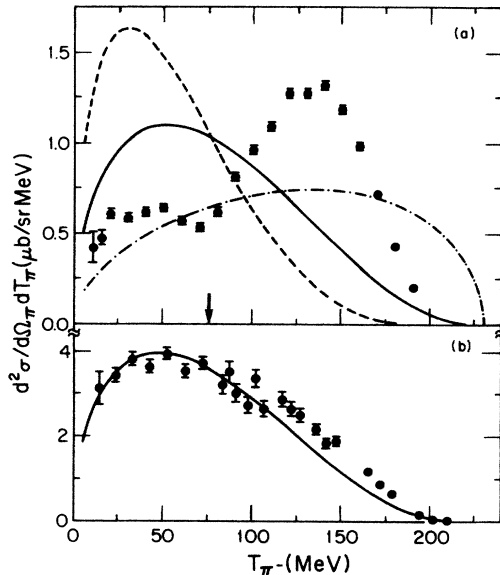


FIG. 1. Doubly differential cross sections for the reactions (a) ${}^4\text{He}(\pi^+, \pi^-)4p$ and (b) ${}^{16}\text{O}(\pi^+, \pi^-)X$ at incident energy 240 MeV and laboratory angle 25° . The dashed and dot-dashed curves in (a) correspond to the distribution of events in five-body and three-body phase space, respectively, while the solid curves in (a) and (b) correspond to four-body phase space (see Ref. 13). The arrow in (a) indicates the maximum pion energy allowed in pion-induced pion production.

${}^{16}\text{O}(\pi^+, \pi^-)X$ at the same energy and angle¹¹ is shown in Fig. 1(b). The two spectra are seen to have strikingly different shapes; the ${}^4\text{He}$ spectrum contains a prominent peak at $T_{\pi^-} \approx 130$ MeV which is absent in the ${}^{16}\text{O}$ spectrum. Figure 2 displays the angular variation of the outgoing pion spectrum at 240-MeV incident energy, while the dependence on incident energy of the 25° spectrum is shown in Fig. 3. The 150-MeV spectrum at 25° contains the first hint of the high-energy feature; it is clear at 180 MeV and is most evident at 240 MeV. At 270 MeV, the low-energy strength is much larger relative to the high-energy peak. Some of this effect could result from pion-induced pion production which yields pions of up to 105-MeV kinetic energy at this angle. As seen in Fig. 2, the energy of the high-energy peak is approximately half the incident energy at 25° and decreases with increasing pion angle. However, the variation of the centroid of the peak with respect to angle and incident energy was found not to correspond to that of a resonance with constant invariant mass.

The energy spectra measured in the reaction ${}^4\text{He}(\pi^-, \pi^+)4n$ at 180 and 240 MeV are very similar at all angles to those measured in the reaction ${}^4\text{He}(\pi^+, \pi^-)4p$. As an example, the π^\pm spectra at 240 MeV and 50° are compared in Fig. 4.

A peak at high outgoing pion energy has been observed^{14,15} at forward angles in the doubly differential cross section for inclusive DCX in ${}^3\text{He}$. A similar peak

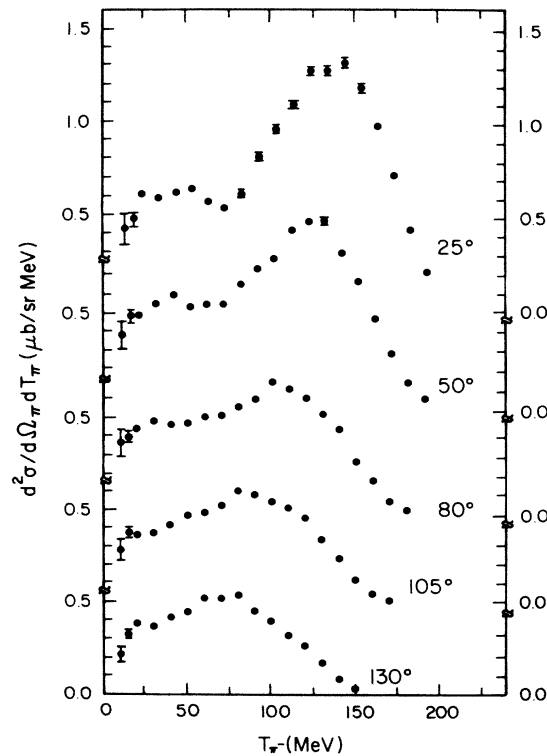


FIG. 2. Doubly differential cross sections for the reaction ${}^4\text{He}(\pi^+, \pi^-)4p$ for incident energy 240 MeV, at laboratory angles $25^\circ, 50^\circ, 80^\circ, 105^\circ,$ and 130° .

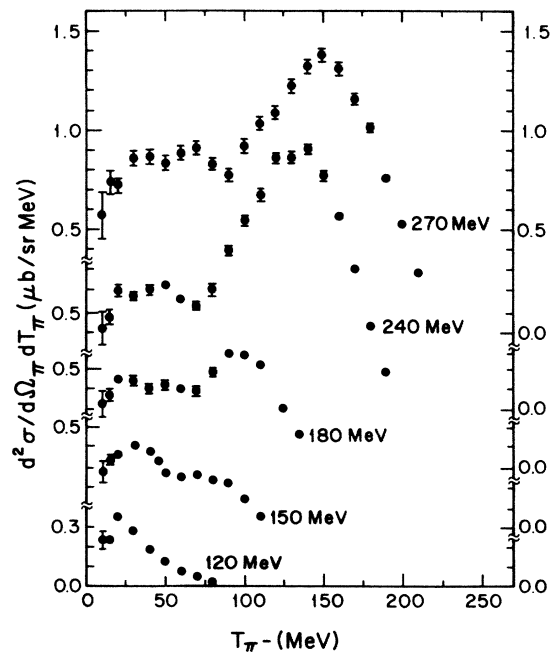


FIG. 3. Doubly differential cross sections for the reaction ${}^4\text{He}(\pi^+, \pi^-)4p$, at laboratory angle 25° , for incident pion energies of 120, 150, 180, 240, and 270 MeV.

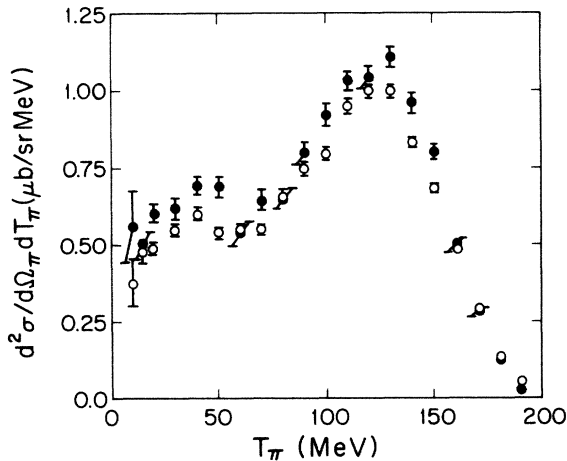


FIG. 4. Doubly differential cross sections for the reactions ${}^4\text{He}(\pi^+, \pi^-)4p$ (solid circles) and ${}^4\text{He}(\pi^-, \pi^+)4n$ (open circles) at incident energy 240 MeV and laboratory angle 50° .

in ${}^4\text{He}$ was not previously seen,^{7,9,15} presumably because of the limited range of the observations and the statistical accuracy of the data. A calculation¹⁶ for ${}^3\text{He}$ demonstrated that final-state interactions among the recoiling (low-energy) nucleons could account for the enhanced high-energy cross section.

In an attempt to explain the Bactrian character of the ${}^4\text{He}$ spectra, one might first examine the distributions of events in phase space for some possible final states.¹³ In Fig. 1(a), the distributions for the reactions $\pi^+ + {}^4\text{He} \rightarrow \pi^- + p + p + p + p$ (dashed curve), $\pi^+ + {}^4\text{He} \rightarrow \pi^- + (2p) + p + p$ (solid curve), and $\pi^+ + {}^4\text{He} \rightarrow \pi^- + (3p) + p$ (dot-dashed curve) are compared with the measured spectrum. The three-body and four-body distributions indicate the effect upon the phase space if two- or three-nucleon "clusters" are formed in the DCX process. It is clear that none of these distributions even approximately represents the data. This is in contrast to the ${}^{16}\text{O}$ case: In Fig. 1(b) the distribution for the reaction $\pi^+ + {}^{16}\text{O} \rightarrow \pi^- + {}^{14}\text{O} + p + p$ is compared with the data. The strong resemblance between the four-body phase-space distribution and the observed energy spectra persists throughout a broad range of incident pion energies and outgoing-pion angles,¹¹ although the shapes do not always match as well as in this illustration.

Since simple phase-space arguments alone cannot explain the shape of the measured spectra for ${}^4\text{He}$, one may next ask whether there is an alternative simple dynamical explanation. As a consequence of the dominantly p -wave π - N interaction at the energies of this experiment, each scattering in the sequential single-charge-exchange (SCX) model of DCX will have a cross section proportional to $1 + 3\cos^2\theta$. For DCX pions emerging at forward angles, this angular distribution will favor either two small-angle scatterings, resulting in small pion energy loss, or two large-angle scatterings, re-

sulting in large energy loss, thus producing the doubly peaked energy spectra that are observed.

Two semiclassical models have incorporated this idea. Thies¹⁷ has convoluted two quasielastic-scattering cross sections, with the nucleons in ${}^4\text{He}$ described by Gaussian wave functions, and obtains doubly peaked spectra with kinematic trends similar to those of the present data. However, neither the shapes nor the relative heights of the peaks match those observed. Wood¹¹ has performed calculations for DCX in ${}^{16}\text{O}$, assuming a Fermi distribution for the nucleon momenta. A two-step SCX calculation, similar in spirit to that of Thies, also yields a doubly peaked spectrum at forward angles; the high-energy peak is accentuated if Pauli blocking is ignored. In an intranuclear cascade calculation, which allows competing processes such as noncharge-exchange scattering and absorption to occur, the high-energy peak is strongly suppressed; the outgoing pion yield is found mainly at low energies, in rough qualitative agreement with the ${}^{16}\text{O}$ data. This suggests that sequential SCX may be the principal mechanism operating in inclusive DCX; its signature is seen clearly in ${}^4\text{He}$ but is masked by higher-order multiple scattering and absorption in ${}^{16}\text{O}$.

The two most recent microscopic calculations^{2,3} of the intermediate-energy DCX process find markedly different results. In Ref. 2, the authors have examined a sequential SCX model for the reaction in ${}^4\text{He}$ using several different forms for the ground-state wave function, as well as taking the proper antisymmetrization of the final state into account, but including only a crude estimate of the final-state interactions. The results are generally much smaller in magnitude than any of the reported ${}^4\text{He}$ data, with the exception of the measurement of Kaufman *et al.*,⁹ which now appears to be low by a factor of 10^2 (see Ref. 7).

In the calculations of Ref. 3, the momentum wave functions of the nucleons are expanded in a basis of hyperspherical functions and the initial and final states are derived from NN potentials, thereby guaranteeing orthogonality as well as accounting for final-state interactions in a more nearly complete fashion than in the calculation of Ref. 2. These authors³ also consider a sequential SCX reaction model, and in addition treat the pion-pion (cloud) scattering mechanism.⁴ This calculation³ obtains fair agreement with the doubly differential cross sections measured at forward angles for DCX in ${}^3\text{He}$ at 140 MeV (Ref. 14) and ${}^4\text{He}$ at 295 MeV (Ref. 7). The inclusion of final-state interactions appears to be crucial to the explanation of the data and some sensitivity to the choice of NN potential is found. A comparison of the predictions of the calculations of both Refs. 2 and 3 with the present data would be most interesting.

In summary, we have shown here samples of an extensive collection of measurements of cross sections for inclusive DCX in ${}^4\text{He}$ for incident pion energies between 120 and 270 MeV, and have offered a qualitative explanation for the surprising spectra observed. Quantita-

tive understanding of these cross sections must await further theoretical work.

This work was supported in part by the U.S. Department of Energy.

^(a)Present address: Tel Aviv University, Ramat Aviv, Tel Aviv, Israel.

¹F. Becker and Yu. A. Batusov, Riv. Nuovo Cimento **1**, 309 (1971).

²W. R. Gibbs *et al.*, Phys. Rev. C **15**, 1384 (1977).

³R. I. Jibuti and R. Ya. Kezerashvili, Nucl. Phys. **A437**, 687 (1985); R. I. Dzhibuti and R. Ya. Kezerashvili, Sov. J. Nucl. Phys. **34**, 810 (1981).

⁴J. F. Germond and C. Wilkin, Lett. Nuovo Cimento **13**, 605 (1975).

⁵J. B. Jeanneret, M. Bogdanski, and E. Jeannet, Nucl. Phys. **A350**, 345 (1980).

⁶J. E. Unger *et al.*, Phys. Lett. **144B**, 333 (1984); R. E. P. Davis *et al.*, Bull. Am. Phys. Soc. **9**, 627 (1964); L. Gilly *et al.*,

Phys. Lett. **19**, 335 (1965).

⁷A. Stetz *et al.*, Phys. Rev. Lett. **47**, 782 (1981).

⁸N. Carayannopoulos *et al.*, Phys. Rev. Lett. **20**, 1215 (1968); I. V. Falomkin *et al.*, Lett. Nuovo Cimento **16**, 525 (1976).

⁹L. Kaufman *et al.*, Phys. Rev. **175**, 1358 (1968).

¹⁰S. A. Wood *et al.*, Phys. Rev. Lett. **54**, 635 (1985).

¹¹S. A. Wood, Los Alamos National Laboratory Report No. LA-9932-T, 1983 (unpublished).

¹²P. J. Bussey *et al.*, Nucl. Phys. **B58**, 363 (1973); J. B. Walter and G. A. Rebka, Jr., Los Alamos National Laboratory Report No. LA-7731-MS, 1979 (unpublished).

¹³The four-body distribution for ¹⁶O has been normalized so that the total volume in phase space is equal to the total DCX cross section. All the distributions shown for ⁴He have been normalized to give the total cross section one would expect from a simple scaling model suggested by Wood (see Ref. 11).

¹⁴J. Sperinde *et al.*, Nucl. Phys. **B78**, 345 (1974).

¹⁵A. Stetz *et al.*, Nucl. Phys. **A457**, 669 (1986).

¹⁶A. C. Phillips, Phys. Lett. **33B**, 260 (1970).

¹⁷M. Thies, private communication.